Ex. 1

DET NORSKE VIDENSKAPS-AKADEMI I OSLO

GEOFYSISKE PUBLIKASJONER

GEOPHYSICA NORVEGICA

Vol. XXVI. No. 2 February 1965

WILLIAM BLUMEN

A random model of momentum flux by mountain waves

OSLO 1965

UNIVERSITETSFORLAGET

GEOFYSISKE PUBLIKASJONER
GEOPHYSICA NORVEGICA

VOL. XXVI. NO. 2

A RANDOM MODEL OF MOMENTUM FLUX BY MOUNTAIN WAVES

BY WILLIAM BLUMEN[1]
Institute of Theoretical Meteorology, University of Oslo

FREMLAGT I VIDENSKAPS-AKADEMIETS MØTE DEN 11TE SEPTEMBER 1964 AV ELIASSEN

Summary. The vertical flux of horizontal momentum produced by small-amplitude steady-state internal gravity waves, generated by flow over a line of mountains in an inviscid adiabatic nonrotating atmosphere, is investigated. The mountain amplitudes and deviations from a constant mean spacing are treated as random variables with rectangular probability distributions and the following effects are investigated: (1) interactions between wave disturbances generated by neighboring mountains, (2) the effect of an upper stable layer, e.g., a stratosphere, (3) the orientation of the mountains relative to the basic current.

The results show that the effect produced by the interactions depends on whether the mean mountain spacing is less or greater than the shortest internal gravity wave. However with increasing randomness in the mountain spacing and/or increasing distance between mountains the effect of the interactions diminishes. In general an upper layer with a high static stability (e.g., a stratosphere), reduces the stress below the value in a reference isothermal atmosphere. An exception may occur when a wave, whose horizontal length is in phase with the mean mountain spacing, has a vertical wave length which is in phase with the interface (or tropopause) height. Other conditions being equal the greatest stress arises from flow over a ridge or line of closely spaced mountains oriented crosswind; and the maximum value occurs when the principal Fourier components of the mountain (or ridge) coincide with those of the wave solution.

CONTENTS

	Page
1. Introduction	2
2. First-order system of equations	3
2.1 Differential equation	3
2.2 Boundary conditions	4
3. The drag: method of solution	5
4. The model	6
4.1 Finite number of mountains	6
4.2 Limit for $N \to \infty$	12

[1] Now at the National Center for Atmospheric Research, Boulder, Colorado.

5. Expected value of the stress in a two-layer model 15
6. Expected value of the stress in a three-dimensional atmosphere 21
6.1 Mountains oriented parallel to the basic current 21
6.2 Mountains oriented crosswind 26
7. Concluding remarks 28
Acknowledgements 29
Appendices 30
Principal symbols used 31
References 32

1. Introduction. Attention has been directed recently to the importance of internal gravity-wave motion as a mechanism for the transport of energy and momentum within the atmosphere. HINES (1960, 1963) has proposed that many of the observed irregular motions in the upper atmosphere, particularly at meteor heights (approximately 80-115 km above the earth), may be interpreted on the basis of internal gravity-wave motion. He suggested that these waves, originating from disturbances in the lower atmosphere, propagate upward undergoing a selective reflection and refraction which depends on the large-scale wind and temperature distribution throughout the atmosphere. ELIASSEN and PALM (1961) have investigated the concept of reflection and transmission of steady-state internal gravity-wave motion generated by flow over small-scale orography. This gravity-type mountain wave transports wave energy upward from the source (the mountain) while its phase progression is downward. As a consequence momentum is transported toward the mountain from aloft. SAWYER (1959) has estimated that this vertical momentum flux (or stress), arising from gravity-type disturbances, is the same order of magnitude as the surface frictional stress under similar conditions of wind and temperature. SAWYER's estimate was based on a simple two-dimensional model in which the parameter $\beta^2 = gu_0^{-2} d\ln\theta_0/dz$ was assumed constant throughout the atmosphere.

In this paper the flux of momentum by internal gravity waves, generated by a line of mountains of irregular amplitude and spacing, will be investigated. We shall primarily be concerned with the effects produced by:

(1) the interactions between wave disturbances generated by neighboring mountains,
(2) a stable upper layer, e.g., a stratosphere,
(3) the orientation of the mountains relative to the basic current in a three-dimensional atmosphere.

The stress at the surface will be computed by a method similar to that used by SAWYER (1959), who also made a rough estimate of its variation with height. However it is sufficient to study only the constant stress exerted on the atmosphere by the ground since ELIASSEN and PALM (1961) have shown that, when internal momentum sources are absent (e.g. rotation, friction), the stress is independent of height in layers where the basic current does not vanish. In order to apply small perturbation theory we shall assume that the characteristic ratio of the mountain height to its breadth is of order 10^{-1} and that all the air flows over the mountain. Our results therefore will be of limited value, since the blocking effects of steep mountains is not taken into account. However the linear analysis is mathematically tractable and serves as a useful introduction to more realistic models.

2. First-order system of equations.

2.1 Differential equation. The system of first-order or perturbation equations governing inviscid and isentropic flow in a stratified rotating atmosphere has been derived by QUENEY (1947). QUENEY's equations will be modified by making the following additional assumptions:

(1) The basic motion u_0 which flows parallel to the x-axis may depend upon height z but is otherwise uniform in space and time.

(2) Only disturbances of small horizontal scale ($L \sim 10$ km) unaffected by the earth's rotation will be considered.

With a change in notation QUENEY's equations may be written in the following form:

$$u_0\frac{\partial u}{\partial x}+w\frac{du_0}{dz}=-\frac{\partial p}{\partial x} \tag{2.1}$$

$$u_0\frac{\partial v}{\partial x}=-\frac{\partial p}{\partial y} \tag{2.2}$$

$$u_0\frac{\partial w}{\partial x}=-\left(\frac{\partial}{\partial z}+\Gamma\right)p+\theta g \tag{2.3}$$

$$u_0\frac{\partial}{\partial x}\frac{p}{c_0^2}+\frac{\partial u}{\partial x}+\frac{\partial v}{\partial y}+\left(\frac{\partial}{\partial z}-\Gamma\right)w=0 \tag{2.4}$$

$$u_0\frac{\partial \theta}{\partial x}+w\frac{d}{dz}\ln\theta_0=0 \tag{2.5}$$

If we denote zero- and first-order quantitites by the subscripts zero and one respectively then:

(u,v,w) $=\rho_0^{1/2}(u_1,v_1,w_1)$, where ρ_0 is the density and (u_1,v_1,w_1) are the components of velocity in a rectangular Cartesian coordinate system

p $=\rho_0^{-1/2}p_1$, where p_1 is pressure

θ $=\rho_0^{1/2}\theta_1\theta_0^{-1}$, where θ_n is potential temperature

Γ $=gc_0^{-2}+1/2d\ln\rho_0/dz$, where g is the acceleration of gravity and

c_0 $=(c_p p_0/c_v\rho_0)^{1/2}$ is the adiabatic sound speed, assumed constant; and c_p/c_v is the ratio of the specific heats.

We shall assume that the first-order variables may be expressed by Fourier integrals of the form

$$w(x, y, z) = \int_{-\infty}^{\infty}\int_{-\infty}^{\infty} W(z; k, l) e^{i(kx+ly)} dl dk . \tag{2.6}$$

Then taking the Fourier transform of equations (2.1) through (2.5) and eliminating all the variables but W, we obtain the following equation

$$\frac{d^2 W}{dz^2} + \frac{k'^2 + l^2}{k'^2}\left[\beta'^2 - k'^2\left(1 + \frac{\frac{1}{u_0}\frac{d^2 u_0}{dz^2} + 2\Gamma\frac{d\ln u_0}{dz} + \frac{d\Gamma}{dz} + \Gamma^2}{k'^2 + l^2}\right)\right] W = 0 . \tag{2.7}$$

Here $(k'^2, \beta'^2) = (1 - u_0^2/c_0^2)(k^2, \beta^2)$, where $\beta^2 = g u_0^{-2} d\ln\theta_0/dz$. Since $u_0^2/c_0^2 \ll 1$ and the terms containing Γ are much smaller than β^2 (2.7) may be simplified to

$$\frac{d^2 W}{dz^2} + \frac{k^2 + l^2}{k^2}\left[\beta^2 - k^2\left(1 + \frac{\frac{1}{u_0}\frac{d^2 u_0}{dz^2}}{k^2 + l^2}\right)\right] W = 0 . \tag{2.8}$$

CRAPPER's (1959) equation (31) is equivalent to (2.8) except for small terms containing the zero-order density. However (2.8) is a more convenient form in this investigation, since it incorporates the transformation $\rho_0^{1/2} W_1$.

2.2 The boundary conditions. The kinematic boundary condition at the earth's surface is, to first-order,

$$w(x, y, 0) = \rho_0^{1/2} u_0 \partial h(x, y)/\partial x, \qquad z = 0 \tag{2.9}$$

where $h(x,y)$ denotes ground profile.

In this investigation we shall only treat atmospheric models which make the coefficients in (2.8) constant. Therefore in an unbounded upper layer it is possible to use the condition derived by ELIASSEN and PALM (1961), which eliminates the solution transporting energy downward from infinity,

$$(pw)_{ave} > 0 , \qquad z \to \infty \tag{2.10}$$

where $(\ )_{ave}$ denotes an average over one wave length.

In the case of two-dimensional motion $(\partial/\partial y \equiv 0)$, an interface between two layers will be defined as a discontinuity in the parameter

$$l^2 = \beta^2 - \frac{1}{u_0}\frac{d^2 u_0}{dz^2} = \text{constant} . \tag{2.11}$$

Then if we assume that u_0 and ρ_0 are continuous across the interface, the kinematic and dynamic boundary conditions require the continuity of vertical velocity and pressure respectively. Following ELIASSEN and PALM (1961) we shall assume that these conditions can be approximated by requiring that at the interface

$$w \text{ and } dw/dz^{(1)} \text{ continuous}. \tag{2.12}$$

Conditions (2.9) and (2.10), and (2.12) when applicable, suffice to determine a unique solution of (2.8).

3. The drag: method of solution. The total x-component of the force or drag exerted on the atmosphere by the ground due to the first-order motion is denoted by

$$D_x = -\iint_A uw\,dx\,dy = \overline{uw} \tag{3.1}$$

where the limits of integration are defined by the horizontal extent of the disturbance. A similar definition holds for the y-component, D_y. Later it will be mathematically expedient to extend the limits of integration to $\pm\infty$, but this does not violate our scale considerations since the disturbance is assumed to be restricted to the area A. SAWYER (1959) has computed the surface drag (3.1) for the case of a constant basic current flowing over a two-dimensional ridge in an isothermal atmosphere. We shall present a more general method to compute (3.1). This method may also be used, for example, to compute the drag as a function of height when rotation and/or friction are added to the problem. The method will be illustrated by rederiving SAWYER's expression, but its application to other models is straight forward.

The differential equation (2.8) reduces to

$$\frac{d^2W}{dz^2} + (\beta^2 - k^2)W = 0 \tag{3,2}$$

The solution which satisfies (2.9) and (2.10) is

$$w(x,z) = \rho_0^{1/2} u_0 Re \frac{\partial}{\partial x}\int_0^\infty F(k) e^{i(kx+\lambda z)} dk \equiv Re \frac{\partial}{\partial x}\int_0^\infty \mathscr{F}(x,z;k)\,dk \tag{3.3}$$

where $F(k)$ is the Fourier transform of $h(x)$ and $\lambda^2 = \beta^2 - k^2$. Next the continuity equation (2.4) is used to determine $u(x,z)$. However to be consistent with the derivation of (2.8) the terms containing c_0^2 and Γ in (2.4) will be neglected. Now we form the product

$$-Reu Rew = -\tfrac{1}{4}\int_0^\infty\int_0^\infty [\lambda\mathscr{F}(k) - \lambda^*\mathscr{F}^*(k)] \times \xi[\mathscr{F}(\xi) - \mathscr{F}^*(\xi)]\,d\xi\,dk \tag{3.4}$$

where $(\lambda^*, \mathscr{F}^*)$ denote the complex conjugates of $(\lambda, \mathscr{F})$ and ξ is a dummy variable.

Next we integrate over x, changing the order of integration and extending the limits of integration to $\pm\infty$ to take advantage of relationships of the form (SNEDDON, 1951)

[1] The latter relation has been derived from the dynamic condition by neglecting the jump in du_0/dz across the interface, which is assumed small.

$$2\pi\delta(\xi-k)=\int_{-\infty}^{\infty} e^{i(\xi-k)x}dx\,. \tag{3.5}$$

$\delta(\xi-k)$ is the Dirac delta function, which has the property that

$$\int_{-\infty}^{\infty} f(\xi;k)\delta(\xi-k)d\xi=f(k)\,. \tag{3.6}$$

The range of integration need not be from $-\infty$ to $+\infty$ but may be over any domain surrounding the point k at which the delta function does not vanish.

Making use of (3.5) and (3.6) we obtain

$$D_x=\pi\rho_0 u_0^2\int_0^{\beta}|F(k)|^2k\sqrt{\beta^2-k^2}dk \tag{3.7}$$

since all the terms containing z cancel. Comparing (2.7) to (2.8) we see that the form of (3.7) would be unaltered, except for a suitable redefinition of β and k, if the terms containing Γ and c_0^2 had been retained.

4. The Model. When there are a number of mountains over a finite area the drag will be affected by interactions between neighboring wave disturbances. If the mountains are far apart the interactions will not be important since the wave amplitudes would have damped considerably before reaching the next mountain downstream. When the topography is composed of tightly spaced ridges, for example, phase relationships exist between neighboring wave disturbances. In subsequent sections these remarks will be illustrated by considering various atmospheric models in which the earth's topography will be represented by a number of mountains whose amplitude and spacing are random variables. The procedure followed is an application of a method used by MACFARLANE (1949) to investigate the noise arising from the fluctuations in the repetition rate and amplitude of a succession of pulses.

4.1. Finite number of mountains. This model consists of an isothermal atmosphere flowing at a constant velocity over a finite number of ridges, each extending infinitely far in the y-direction (crosswind). The total x-distance between the first and last ridge is assumed small enough so that the earth's rotation and horizontal variations in the basic current may be neglected. Then the drag exerted on the atmosphere by the ground may be computed from (3.7) when $F(k)$ is specified.

Suppose the vertical velocity at the earth's surface is represented by $N+1$ doublets of equal strength a distance η apart; then the surface is composed of $N+1$ point deformations of finite cross-sectional area aL and

$$F_n(k)=\frac{aL}{\pi}\sum_{n=0}^{N} e^{-ink\eta} \tag{4.1}$$

where the product of the amplitude a and length L also measures the doublet strength. It follows that

(4.2)
$$|F_n(k)|^2 = \left(\frac{aL}{\pi}\right)^2 \left|\sum_{n=0}^{N} e^{-ink\eta}\right|^2 =$$
$$(N+1) + 2N\cos k\eta + 2(N-1)\cos 2k\eta + \cdots + 2\cos Nk\eta$$

which may be proved by induction. When (4.2) is substituted into (3.7) the drag becomes

(4.3)
$$D_x = \rho_0 u_0^2 a^2 L^2 \pi^{-1} \int_0^{\beta} k\sqrt{\beta^2 - k^2} \times$$
$$[(N+1) + 2N\cos k\eta + 2(N-1)\cos 2k\eta + \cdots + 2\cos Nk\eta]dk\,.$$

The first term in brackets represents the individual contribution to the drag from each of the $N+1$ mountains; the next represents the $2N$ interactions between neighboring mountains, i.e., $(\overline{u_0 w_1} + \overline{u_1 w_0}) + (\overline{u_1 w_2} + \overline{u_2 w_1}) + \cdots + (\overline{u_{N-1} w_N} + \overline{u_N w_{N-1}})$. The remaining terms are interpreted similarly. It should be noted that since $|F_n(k)|^2 \geqslant 0$, the interaction terms cannot produce a net upward flux of momentum from the surface.

In general if we assume that there are $N+1$ mountains of different sizes and shapes not spaced the same distance from each other, then

(4.4)
$$|F_n(k)|^2 = \left|\sum_{n=0}^{N} H_n(k) e^{-ik(n\eta + \phi_n)}\right|^2$$

where $H_n(k)$ is the Fourier transform and $n\eta + \phi_n$ the position of the n^{th} mountain. For the present we shall assume that there are $N+1$ point deformations of equal length L in order to isolate the relative importance of variations in the mountain amplitude and spacing. Then

(4.5)
$$H_n(k) = a_n L/\pi$$

To estimate the effect produced by a variety of different spacings we shall assume that the deviation ϕ from the mean spacing η is a random variable with a mean of zero and a probability distribution $p(\phi)$. A mean or expected value of $f(\phi)$ is defined as

(4.6)
$$\{f(\phi)\}_{ave} = \int_{\phi_{min}}^{\phi_{max}} f(\phi) p(\phi) d\phi$$

where the limits of integration extend over the range of ϕ.

Similarly the amplitude a_n is expressed as a constant mean value $\tilde{a}$ plus a deviation:

(4.7)
$$a_n = \tilde{a} + (a_n - \tilde{a})$$

where

(4.8)
$$\tilde{a} = \int_{a_{min}}^{a_{max}} a q(a) da$$

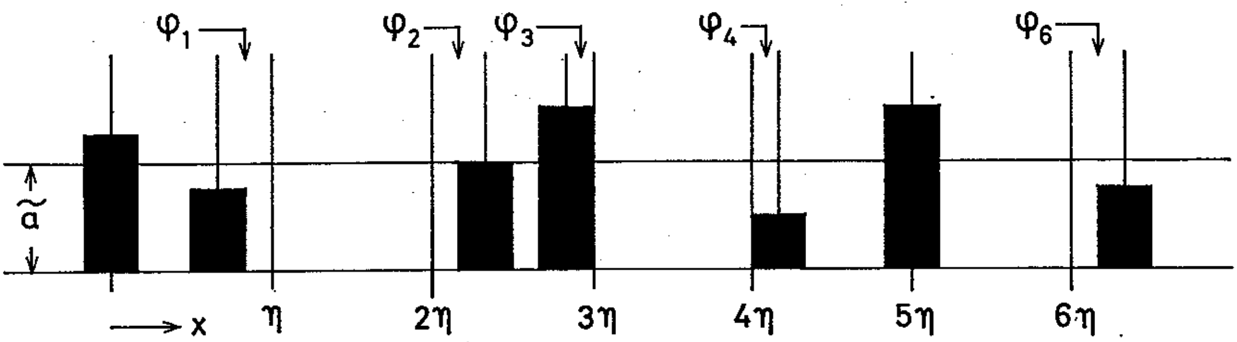

Fig. 1. A schematic representation of a line of point deformations with irregular amplitudes and spacing. $\tilde{a}$ denotes the mean amplitude and φ_n represents the deviation from the mean spacing η.

and $q(a)$ is the probability distribution of a. The model is shown schematically in Fig. 1.

The probability distributions $p(\phi)$ and $q(a)$ could be estimated for different mountainous regions. This will not be done here since the model is not realistic enough in other respects to warrant a more precise determination of these distributions. Rather the purpose is to see if the choice of distribution is a critical factor in the model and to obtain some quantitative information concerning the stress when the mountains are distributed in random manner.

The form of the probability distributions is limited by the fact that the variations in the amplitude and in the deviations from the mean spacing are bounded. The simplest continous distribution which may be used to satisfy these criteria is a rectangular distribution. This implies that all values of the amplitude and spacing occur with equal probability within their respective ranges of variation. The reason for using the rectangular distribution is to introduce as much randomness as possible. This will provide one limiting value for the stress, the case of equal spacing ($\phi_n \equiv 0$) and constant amplitude ($a_n \equiv \tilde{a}$) the other. If we had reason to believe that small-scale mountains are usually spaced close to some mean value then a triangular type probability distribution might be more realistic.

The probability distribution for the deviation from the mean spacing is

$$p(\phi) = 1/2\alpha \qquad \text{when} \qquad |\phi| \leq \alpha \tag{4.9}$$

and

$$p(\phi) = 0 \qquad \text{when} \qquad |\phi| > \alpha \tag{4.10}$$

where α is the maximum distance from the central point $n\eta$. Likewise the probability distribution of the individual mountain amplitudes is

$$q(a) = 1/(a_2 - a_1) \qquad \text{when} \qquad a_1 \leq a \leq a_2 \tag{4.11}$$

and

$$q(a) = 0 \qquad \text{when} \qquad a < a_1 \qquad \text{or} \qquad a > a_2 \tag{4.12}$$

where $a_2 - a_1$ is the range of amplitudes permitted in the model.

Using (4.4) through (4.8) the expected value of the drag is given by

$$\{\widetilde{D_x}\}_{ave}=\pi\rho_0 u_0^2 \int_0^\beta \{|\widetilde{F_n(k)}|^2\}_{ave} k\sqrt{\beta^2-k^2}\,dk\,. \tag{4.13}$$

The indicated averaging process has been carried out in Appendix A with the following result

$$\{|\widetilde{F_n(k)}|^2\}_{ave}=\left(\frac{\tilde{a}L}{\pi}\right)^2\Bigg[\left(\sum_{n=0}^{N}\{\cos k(n\eta+\phi_n)\}_{ave}\right)^2+\left(\sum_{n=0}^{N}\{\sin k(n\eta+\phi_n)\}_{ave}\right)^2$$
$$+\sum_{n=0}^{N}\{\cos^2 k(n\eta+\phi_n)\}_{ave}-\sum_{n=0}^{N}(\{\cos k(n\eta+\phi_n)\}_{ave})^2$$
$$+\sum_{n=0}^{N}\{\sin^2 k(n\eta+\phi_n)\}_{ave}-\sum_{n=0}^{N}(\{\sin k(n\eta+\phi_n)\}_{ave})^2+(N+1)\left(\frac{a-\tilde{a}}{\tilde{a}}\right)^2\Bigg]. \tag{4.14}$$

Using the probability distributions defined by (4.9) through (4.12) we obtain

$$\{|\widetilde{F_n(k)}|^2\}_{ave}=\left(\frac{\tilde{a}L}{\pi}\right)^2\left[\left(\frac{\sin k\alpha}{k\alpha}\right)^2\left[\left(\sum_{n=1}^{N}\sin kn\eta\right)^2+\right.\right.$$
$$\left.\left.\left(\sum_{n=0}^{N}\cos kn\eta\right)^2\right]+(N+1)\left(1-\left(\frac{\sin k\alpha}{k\alpha}\right)^2+\frac{1}{12}\left(\frac{a_2-a_1}{\tilde{a}}\right)^2\right)\right]. \tag{4.15}$$

Substituting (4.15) into (4.13), making the change of variable $k=\beta\xi$ and dividing by the total distance over which the mountains are distributed $N\eta+L$, we obtain the expected value of the stress

$$\{\widetilde{\tau_x}\}_{ave}\equiv\frac{\{\widetilde{D_x}\}_{ave}}{N\eta+L}=\rho_0 u_0^2\tilde{a}^{*2}L^*\pi^{-1}\left(\frac{N+1}{N+L^*/\eta^*}\right)\frac{L^*}{\eta^*}\int_0^1\xi\sqrt{1-\xi^2}\times \tag{4.16}$$
$$\left\{\frac{1}{N+1}\left(\frac{\sin\alpha^*\xi}{\alpha^*\xi}\right)^2[(N+1)+2N\cos\eta^*\xi+2(N-1)\cos 2\eta^*\xi+\cdots+2\cos N\eta^*\xi]+\right.$$
$$\left.+\left[1-\left(\frac{\sin\alpha^*\xi}{\alpha^*\xi}\right)^2\right]+\frac{1}{12}\left(\frac{a_2{}^*-a_1{}^*}{\tilde{a}^*}\right)^2\right\}d\xi$$

where $(a^*, L^*, \alpha^*, \eta^*)=\beta(a, L, \alpha, \eta)$. The contributions to $\{\widetilde{\tau_x}\}_{ave}$ are from: (a) the $N+1$ individual mountains of mean amplitude $\tilde{a}^*$; (b) the interactions between mountains randomly distributed about a mean spacing η^*; (c) the "noise" due to irregularity in spacing and (d) amplitude, which *always* act to increase the drag. We note that terms (a) and (b) differ from the corresponding terms in (4.3) by the factor $(\sin\alpha^*\xi/\alpha^*\xi)^2$ arising from the variability in spacing. The interpretation of this term will be discussed in the following section.

Choosing the characteristic values $gd\ln\theta_0/dz = 4\times10^{-4}$ sec^{-2} and $u_0 = 20$ m sec^{-1}, we obtain $\beta = 1$ km^{-1}. For convenience we shall now drop the asterisks from the non-dimensional variables (a^*, L^*, α^*, η^*) since they are numerically equal to the corresponding dimensional quantities. Since $\xi \leq 1$ we shall assume, for the present, that $\alpha = 1$ (a maximum deviation of ± 1 km from the mean spacing) and make the series expansion

$$\left(\frac{\sin\alpha\xi}{\alpha\xi}\right)^2 = 1 - \frac{1}{3}(\alpha\xi)^2 + \frac{2}{45}(\alpha\xi)^4 - \frac{1}{315}(\alpha\xi)^6 + \cdots \tag{4.17}$$

When (4.17) is introduced into (4.16) integrals of the type

$$\int_0^1 \xi^{2m+1}\sqrt{1-\xi^2}\cos n\eta\xi d\xi\,, \quad (m=0,1,2,\ldots) \tag{4.18}$$

must be evaluated. This may be accomplished by making the transformation $\xi = \cos x$ and using the definition of the Struve function $\boldsymbol{H}_\upsilon(n\eta)$ (Watson, 1944, § 10.45). Next we introduce the stress due to one point deformation, of mean height $\tilde{a} = 0.3$ and length $L = 2\pi$,

$$\tau_x = \frac{\rho_0 u_0^2 \tilde{a}^2 L}{3\pi} = 240 \text{ dynes cm}^{-2} \tag{4.19}$$

as a normalizing factor.[2] Then we obtain the expected value of the stress in nondimensional form

$$E_N(\tau_x) \equiv \frac{\{\tilde{\tau}_x\}_{ave}}{\tau_x} = \tag{4.20}$$

(a)
$$\left(\frac{N+1}{N+L/\eta}\right)\frac{L}{\eta}\left\{\left[1 - \frac{2}{15}\alpha^2 + \frac{16}{1575}\alpha^4 - \cdots\right] + \right.$$

(b)
$$\frac{3\pi}{2(N+1)}\left[2N\left(\frac{\boldsymbol{H}_0(\eta)}{\eta} - 2\frac{\boldsymbol{H}_1(\eta)}{\eta^2}\right) + 2(N-1)\left(\frac{\boldsymbol{H}_0(2\eta)}{2\eta} - 2\frac{\boldsymbol{H}_1(2\eta)}{(2\eta)^2}\right) + \cdots + \right.$$

$$2\left(\frac{\boldsymbol{H}_0(N\eta)}{N\eta} - 2\frac{\boldsymbol{H}_1(N\eta)}{(N\eta)^2}\right) - \frac{\alpha^2}{3}\left[2N\left(\frac{\boldsymbol{H}_0(\eta)}{\eta} - 2\frac{\boldsymbol{H}_1(\eta)}{\eta^2}\right) + \cdots + \right.$$

$$\left.2\left(\frac{\boldsymbol{H}_0(N\eta)}{N\eta} - 2\frac{\boldsymbol{H}_1(N\eta)}{(N\eta)^2}\right)\right] + \alpha^2\left[2N\left(\frac{\boldsymbol{H}_1(\eta)}{\eta^2} - 4\frac{\boldsymbol{H}_2(\eta)}{\eta^3}\right) + \cdots + \right.$$

$$\left.\left.2\left(\frac{\boldsymbol{H}_1(N\eta)}{(N\eta)^2} - 4\frac{\boldsymbol{H}_2(N\eta)}{(N\eta)^3}\right)\right] + \text{ higher order terms}\right] +$$

[2] Although a point deformation is not a realistic profile, since τ_x increases with decreasing u_0, it does serve to bring the important parameters of the problem into focus.

(c)
$$\alpha^2\left[\frac{2}{15}-\frac{16}{1575}\alpha^2+\cdots\right]+$$

(d)
$$\left.\frac{1}{12}\left(\frac{a_2-a_1}{\tilde{a}}\right)^2\right\}.$$

The function $\boldsymbol{H}_\nu(n\eta)$ has been evaluated from ROBINSON's (1948) tables and the contributions to $E_N(\tau_x)$ are presented in Table 1.

From (4.20) we find that the contribution from the individual mountains (a) is positive and approximately equal to L/η. However the interactions, which primarily

Table 1. *Contributions to the expected value of the surface stress $E_N(\tau_x)$. The following numerical values have been used: $L=2\pi$, $a=1$, $a_2-a_1=\tilde{a}=0.3$.*

η	N	5	10	15	20	25
7	a	0.801	0.794	0.792	0.791	0.790
	$a+b$	0.736	0.733	0.733	0.732	0.732
	$a+b+c$	0.848	0.844	0.844	0.843	0.843
	$a+b+c+d$	0.924	0.920	0.919	0.918	0.918
8	a	0.715	0.702	0.698	0.696	0.694
	$a+b$	0.769	0.754	0.749	0.746	0.744
	$a+b+c$	0.869	0.853	0.847	0.844	0.842
	$a+b+c+d$	0.937	0.920	0.913	0.910	0.908
9	a	0.646	0.630	0.624	0.621	0.619
	$a+b$	0.647	0.625	0.617	0.614	0.611
	$a+b+c$	0.736	0.713	0.705	0.701	0.698
	$a+b+c+d$	0.797	0.773	0.764	0.760	0.757
10	a	0.588	0.570	0.564	0.561	0.559
	$a+b$	0.571	0.552	0.546	0.542	0.541
	$a+b+c$	0.653	0.632	0.625	0.621	0.619
	$a+b+c+d$	0.709	0.686	0.679	0.674	0.672
11	a	0.539	0.521	0.515	0.511	0.510
	$a+b$	0.472	0.452	0.445	0.441	0.439
	$a+b+c$	0.548	0.525	0.517	0.513	0.510
	$a+b+c+d$	0.599	0.575	0.566	0.562	0.558
4π	a	0.478	0.460	0.452	0.449	0.447
	$a+b$	0.364	0.339	0.328	0.324	0.322
	$a+b+c$	0.431	0.403	0.392	0.387	0.385
	$a+b+c+d$	0.476	0.447	0.435	0.430	0.427

depend on the phase relationships between neighboring mountains, may transport momentum either upward or downward. This effect can be seen by comparing (a) and (b) in each four-line group. As noted earlier the "noise" terms, (c) and (d), always increase the stress. The computations presented in the Table also show that $E_N(\tau_x)$ is essentially independent of N for $N>10$. This fact enables us to eliminate the variable N by carrying out a limiting procedure, thus simplifying the expression for $E_N(\tau_x)$.

4.2 Limit for $N\to\infty$. Dividing the expression in (4.16) by (4.19) and taking the limit $N\to\infty$, we obtain

$$\lim_{N\to\infty} E_N(\tau_x)=E(\tau_x)= \tag{4.21}$$

$$3\frac{L}{\eta}\int_0^1 \xi\sqrt{1-\xi^2}\left\{\left(\frac{\sin\alpha\xi}{\alpha\xi}\right)^2\left[1+2\sum_{n=1}^{\infty}\cos n\eta\xi\right]+\left[1-\left(\frac{\sin\alpha\xi}{\alpha\xi}\right)^2\right]+\frac{1}{12}\left(\frac{a_2-a_1}{\tilde{a}}\right)^2\right\}d\xi\,.$$

From Lighthill (1959, § 5.4, 43) we have

$$1+2\sum_{n=1}^{\infty}\cos n\eta\xi=\frac{2\pi}{\eta}\sum_{m=-\infty}^{m=\infty}\delta\left(\xi-\frac{2m\pi}{\eta}\right) \tag{4.22}$$

where $\delta(\xi-2m\pi/\eta)$ is the Dirac delta function. Putting (4.22) into (4.21) and carrying out the details of the integration (in Appendix B), we obtain

$$E(\tau_x)= \tag{4.23}$$

(i) $$3\frac{L}{\eta}\left\{\frac{2\pi}{\eta}\sum_{m=0}^{M}\frac{2m\pi}{\eta}\sqrt{1-\left(\frac{2m\pi}{\eta}\right)^2}\left(\frac{\sin\frac{2m\pi\alpha}{\eta}}{\frac{2m\pi\alpha}{\eta}}\right)^2+\right.$$

(ii) $$\int_0^1\xi\sqrt{1-\xi^2}\left[1-\left(\frac{\sin\alpha\xi}{\alpha\xi}\right)^2\right]d\xi+$$

(iii) $$\left.\frac{1}{36}\left(\frac{a_2-a_1}{\tilde{a}}\right)^2\right\}$$

where M is the largest integer satisfying $1-(2M\pi/\eta)^2>0$. Term (i) in (4.23) corresponds to terms (a) and (b) in (4.16); while the noise terms (ii) and (iii) differ from (c) and (d) only by the factor $(N+1/N+L/\eta)\approx 1$.

Suppose, for the moment, that $\alpha=0$, and $\tilde{a}=a$, then

$$E(\tau_x)=3\frac{L}{\eta}\frac{2\pi}{\eta}\sum_{m=0}^{M}\frac{2m\pi}{\eta}\sqrt{1-\left(\frac{2m\pi}{\eta}\right)^2}. \tag{4.24}$$

This expression is the stress due to flow over an infinite number of mountains spaced a mean distance η apart. We first note that if

$$\eta \leq 2\pi = L_s \tag{4.25}$$

the *stress vanishes*. This result means that the interaction terms produce a net upward flux of momentum which exactly cancels the downward flux due to the individual mountains. If $\eta > L_s$, there is a net downward flux of momentum toward the ground.

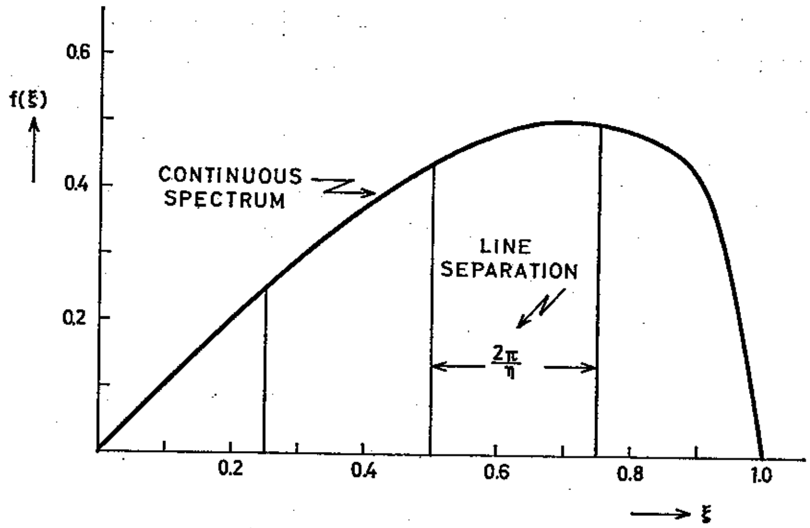

Fig. 2. Continous and line spectrum of internal waves which contribute to the stress for the model described in the text.

The function $f(\xi)=\xi\sqrt{1-\xi^2}$, displayed in Fig. 2, represents the continuous spectrum of internal waves which contribute to the stress. The line spectrum

$$\sum_{m=0}^{M}(2m\pi/\eta)\sqrt{1-(2m\pi/\eta)^2},$$

with envelope $f(\xi)$ and line separation $2\pi/\eta$, corresponds to the discrete number of internal waves which are exactly in phase with the mountain spacing η. For example, if $L_s<\eta\leq 2L_s$, then $M=1$ and there is one internal wave of length η which is exactly in phase with the mountain spacing and reinforcement occurs.[3] A similar argument follows for $M>1$.

[3] If $\eta=2L_s$ the waves of length L_s and $2L_s$ are in phase with the mountain spacing, but we note from Fig. 2 that the stationary wave $L_s(\xi=1)$ does not contribute to the stress.

There is no discrete contribution when (4.25) is satisfied since the critical wave length L_s is the shortest internal wave. Therefore all the internal waves must be out of phase with the mountain spacing and, as noted above, the net effect of the wave interactions is to produce a zero stress.

The significance of the term $(\sin 2m\pi\alpha/\eta/2m\pi\alpha/\eta)^2$ is best illustrated by an example. Suppose $\eta=16$ and $\alpha=4$. This means that each mountain has an equal probability of being located within and including ± 4 km from its mean position. Since $2L_s<\eta<3L_s$ there are two waves of length 8 and 16 km respectively which are exactly in phase with the mean mountain spacing η; but the stress due to the shorter wave is zero since $(\sin\pi/\pi)^2=0$. In other words the shorter wave has a zero probability of being in phase with the mountain spacing, since there is an equal probability that the center of the mountain (the point deformation) is located at any point over a distance equal to 8 km. The contribution from the longer wave is reduced by the factor $(\sin\pi/2/\pi/2)^2$ ≈ 0.4 since the phase relationship is not as pronounced as in the case when $\alpha=0$. It should be noted that this latter effect is distinct from the "noise" due to irregularity in the spacing, given by (ii) in (4.23). The "noise" is continuous and affects the complete spectrum of internal waves.

Table 2. *Contributions to the expected value of the stress $E(\tau_x)$. The same numerical values used in the construction of Table 1 have been taken.*

η	α	1	2	3	4
	i	0.726	0.282	0.252	0.014
7	*i+ii*	0.833	0.640	0.607	0.717
	i+ii+iii	0.908	0.715	0.682	0.792
	i	0.729	0.365	0.081	0.000
8	*i+ii*	0.823	0.678	0.590	0.615
	i+ii+iii	0.889	0.743	0.655	0.680
	i	0.620	0.364	0.125	0.011
9	*i+ii*	0.703	0.642	0.577	0.558
	i+ii+iii	0.762	0.700	0.636	0.616
	i	0.507	0.332	0.147	0.032
10	*i+ii*	0.582	0.582	0.554	0.524
	i+ii+iii	0.634	0.634	0.607	0.576
	i	0.411	0.291	0.153	0.050
11	*i+ii*	0.480	0.519	0.523	0.498
	i+ii+iii	0.527	0.566	0.571	0.545
	i	0.299	0.230	0.144	0.067
4π	*i+ii*	0.359	0.430	0.468	0.459
	i+ii+iii	0.400	0.471	0.509	0.500

The numerical computations of $E(\tau_x)$, given by (4.23), are presented in Table 2. The values in the first column ($\alpha=1$) are the limits which are approached by the corresponding terms in Table 1. The small discrepancies between the values in each table arise primarily because it was necessary to truncate the series in (4.20b) when $N\eta$ reached 25.

As the mountains become more randomly distributed (increasing α) the effect produced by the phase relationship between the wave length and mountain spacing diminishes. At the same time the "noise" component (ii) increases, and when $\alpha=2$ terms (i) and (ii) are approximately equal in magnitude. As α increases further the discrete contribution becomes negligible and the "noise" due to irregularity in the spacing approaches the value

$$E(\tau_x)=L/\eta \tag{4.26}$$

which is the stress due to an infinite number of individual mountains spaced a mean distance η apart. For the range of amplitudes chosen in this model, $a_2-a_1=\tilde{a}$, the "noise" contribution from (iii) is about 10 percent of the sum of (i) and (ii).

5. Expected value of the stress in a two-layer model. Under actual atmospheric conditions the parameter $l^2=\beta^2-u_0^{-1}d^2u_0/dz^2$ is not constant with height. Therefore we shall investigate how a more realistic distribution of l^2 modifies the results presented in Section 4. For this purpose the distribution of l^2, computed by Palm and Foldvik (1960) for a pronounced lee-wave situation, will be approximated by a two-layer atmospheric model. In each layer we assume that

$$l_n^2=(\beta^2-u_0^{-1}d^2u_0/dz^2)_n=\text{constant} \tag{5.1}$$

where $n=1, 2$, referring to the lower and upper layers respectively. Moreover the upper layer is isothermal with a constant basic current and we require that $l_2{}^2\geqslant l_1{}^2$. Since the basic current does not, in general, decrease with height in the lower stratosphere during lee-wave situations the condition $l_2^2>l_1{}^2$ represents an abrupt increase of static stability at the tropopause. As a consequence partial trapping of wave energy takes place in the lower layer, while the energy reaching the top layer is transferred upward by internal wave motion. In all other respects this model is the same as the model in Section 4.

Following the procedure used to derive (4.16) it is possible to derive the expected value of the stress in a two-layer model which satisfies (2.8) through (2.12). The ground is situated at $z=-H$ (H is the mean depth of the lower layer) and we again use $\beta^{-1}=$ 1 km as a unit of length. After a straightforward but lengthy computation we obtain in the lower layer

$$\{\widetilde{\tau_x}\}_{ave} = \frac{\pi \rho_0 u_0^2}{N\eta + L} \times \tag{5.2}$$

$$\left\{ \int_0^{l_1} \{|\widetilde{F_n(\xi)}|^2\}_{ave} \frac{\xi\sqrt{l_2^2-\xi^2}}{1+\varepsilon^2 H^2 \left(\dfrac{\sin\sqrt{l_1^2-\xi^2}H}{\sqrt{l_1^2-\xi^2}H}\right)^2} d\xi + \right.$$

$$\left. \int_{l_1}^{l_2} \{|\widetilde{F_n(\xi)}|^2\}_{ave} \frac{\xi\sqrt{l_2^2-\xi^2}}{1+\varepsilon^2 H^2 \left(\dfrac{\sinh\sqrt{\xi^2-l_1^2}H}{\sqrt{\xi^2-l_1^2}H}\right)^2} d\xi \right\}$$

where $\{|\widetilde{F_n(\xi)}|^2\}_{ave}$ is defined by (4.15), $\varepsilon^2 = l_2^2 - l_1^2$ and $(a, L, H, \alpha, \eta, \xi, l_1, l_2)$ are non-dimensional variables. A similar computation in the upper layer again yields (5.2) because the interface conditions (2.12) imply that the constant stress is continouus across the interface.

The first integral in (5.2) represents the contribution from all the internal waves in the range $0 \leq k \leq l_1$; while the contribution from the internal waves which occur in the upper layer ($l_1 < k \leq l_2$) when external type waves exist below is represented by the second integral. When $l_2 \rightarrow 1$ and either $l_1 \rightarrow l_2$ or $H \rightarrow 0$, (5.2) reduces to (4.16).

We shall again use (4.19) for normalization and take the limit $N \rightarrow \infty$ to obtain

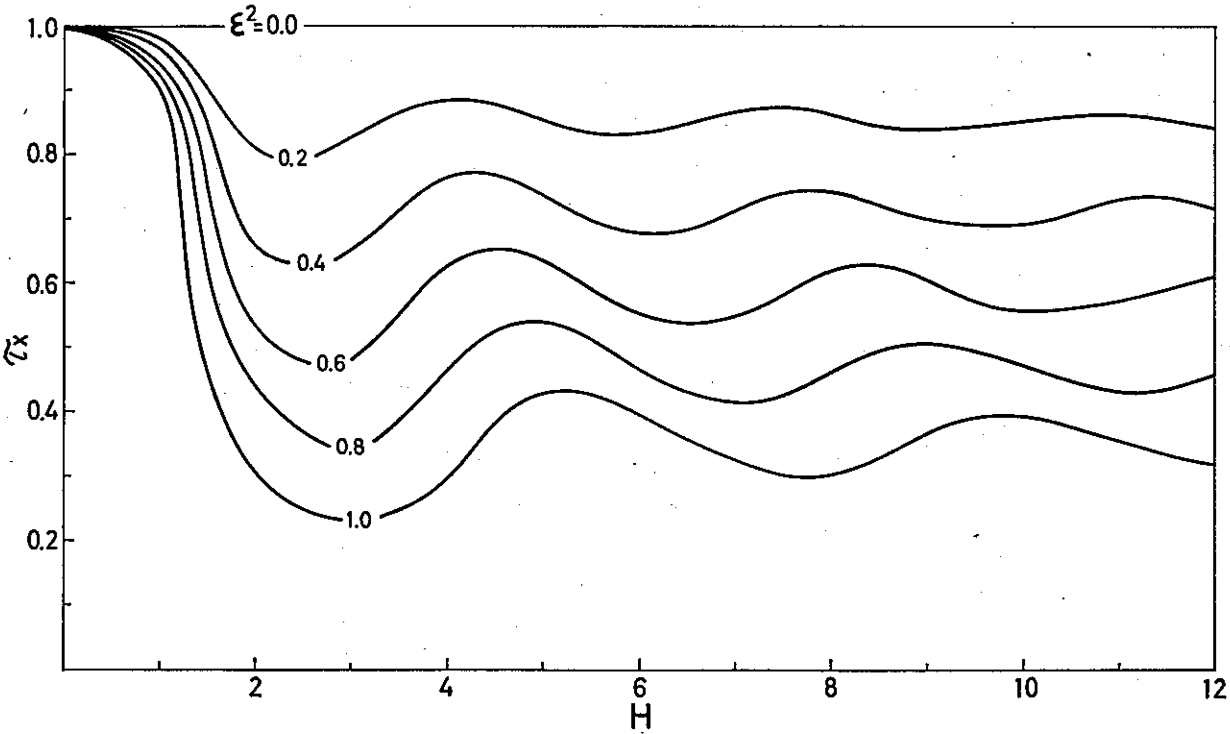

Fig. 3. The stress due to an isolated point mountain as a function of the nondimensional interface height H. Each curve has been drawn for a different constant value of ε^2.

(5.3)

$$E(\tau_x)=$$

$$3\frac{L}{\eta}\left\{\frac{2\pi}{\eta}\sum_{m=0}^{M_1}\frac{\frac{2m\pi}{\eta}\sqrt{l_2^2-\left(\frac{2m\pi}{\eta}\right)^2}\left(\frac{\sin\frac{2m\pi\alpha}{\eta}}{\frac{2m\pi\alpha}{\eta}}\right)^2}{1+\varepsilon^2H^2\left(\frac{\sin\sqrt{l_1^2-\left(\frac{2m\pi}{\eta}\right)^2}H}{\sqrt{l_1^2-\left(\frac{2m\pi}{\eta}\right)^2}H}\right)^2}+\right.$$

$$\int_0^{l_1}\frac{\xi\sqrt{l_2^2-\xi^2}\left[1-\left(\frac{\sin\alpha\xi}{\alpha\xi}\right)^2+\frac{1}{12}\left(\frac{a_2-a_1}{\tilde{a}}\right)^2\right]}{1+\varepsilon^2H^2\left(\frac{\sin\sqrt{l_1^2-\xi^2}H}{\sqrt{l_1^2-\xi^2}H}\right)^2}d\xi+$$

$$\frac{2\pi}{\eta}\sum_{m=M_1+1}^{M_2}\frac{\frac{2m\pi}{\eta}\sqrt{l_2^2-\left(\frac{2m\pi}{\eta}\right)^2}\left(\frac{\sin\frac{2m\pi\alpha}{\eta}}{\frac{2m\pi\alpha}{\eta}}\right)^2}{1+\varepsilon^2H^2\left(\frac{\sinh\sqrt{\left(\frac{2m\pi}{\eta}\right)^2-l_1^2}H}{\sqrt{\left(\frac{2m\pi}{\eta}\right)^2-l_1^2}H}\right)^2}+$$

$$\left.\int_{l_1}^{l_2}\frac{\xi\sqrt{l_2^2-\xi^2}\left[1-\left(\frac{\sin\alpha\xi}{\alpha\xi}\right)^2+\frac{1}{12}\left(\frac{a_2-a_1}{\tilde{a}}\right)^2\right]}{1+\varepsilon^2H^2\left(\frac{\sinh\sqrt{\xi^2-l_1^2}H}{\sqrt{\xi^2-l_1^2}H}\right)^2}d\xi\right\}$$

where M_1 is the largest integer satisfying $l_1^2-(2M_1\pi/\eta)^2>0$ and M_2 must satisfy $l_2^2-(2M_2\pi/\eta)^2>0$. Taking into account the above interpretation of the integrals (and hence the summations) the various terms in (5.3) correspond to the terms in (4.23).

The stress due to an isolated mountain ($N=\alpha=a_2-a_1=0$) has been computed from (5.3) and is presented in Fig. 3. The results show clearly that the upper stable layer *always* acts to decrease the stress below the stress in an unbounded isothermal atmosphere, $E(\tau_x)=1$. This occurs because vertical motion is inhibited at the interface

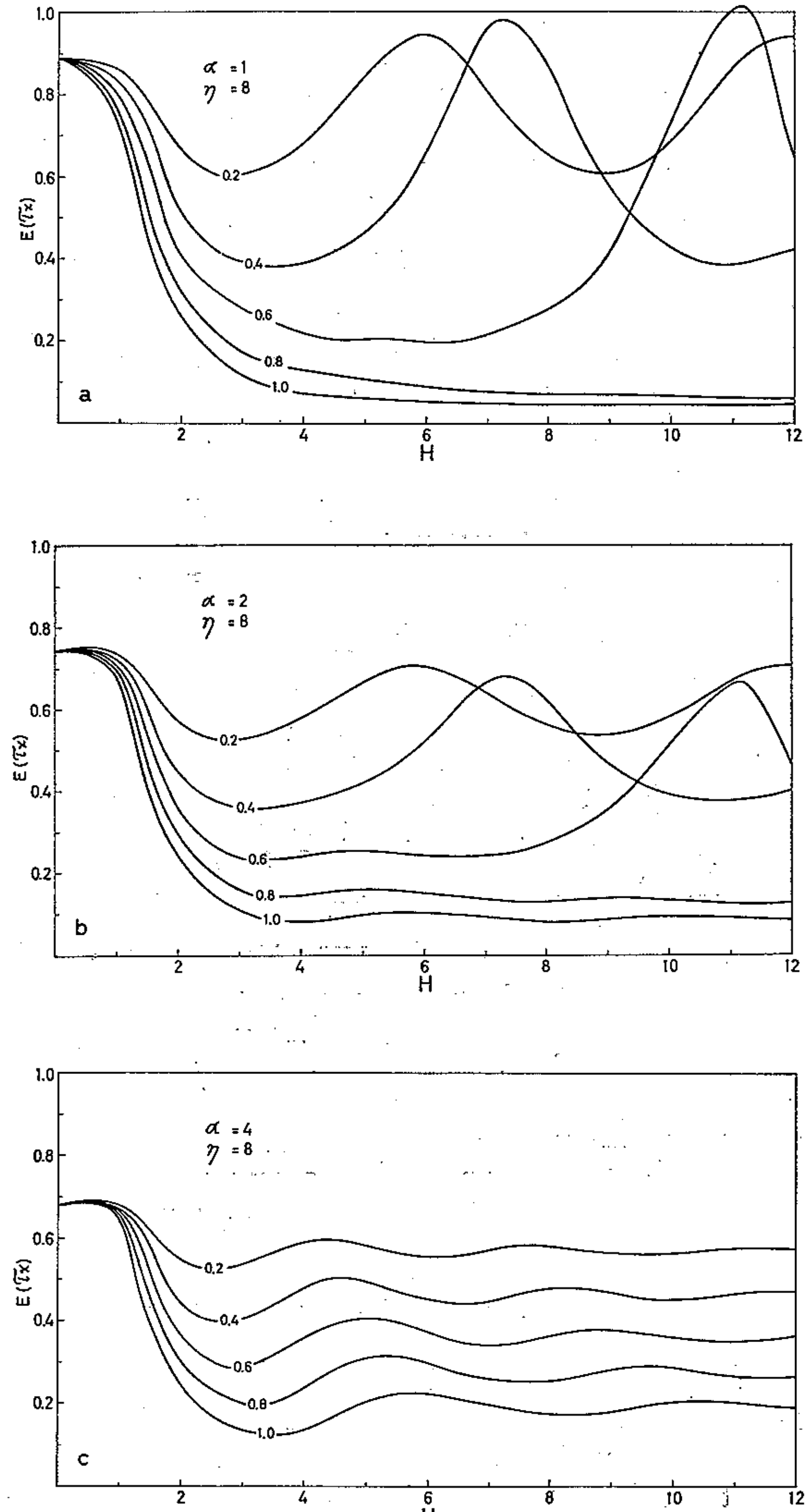

Fig. 4. The expected value of the stress as a function of H for the indicated values of mean spacing η and deviation α. Each curve represents a different constant value of ε^2.

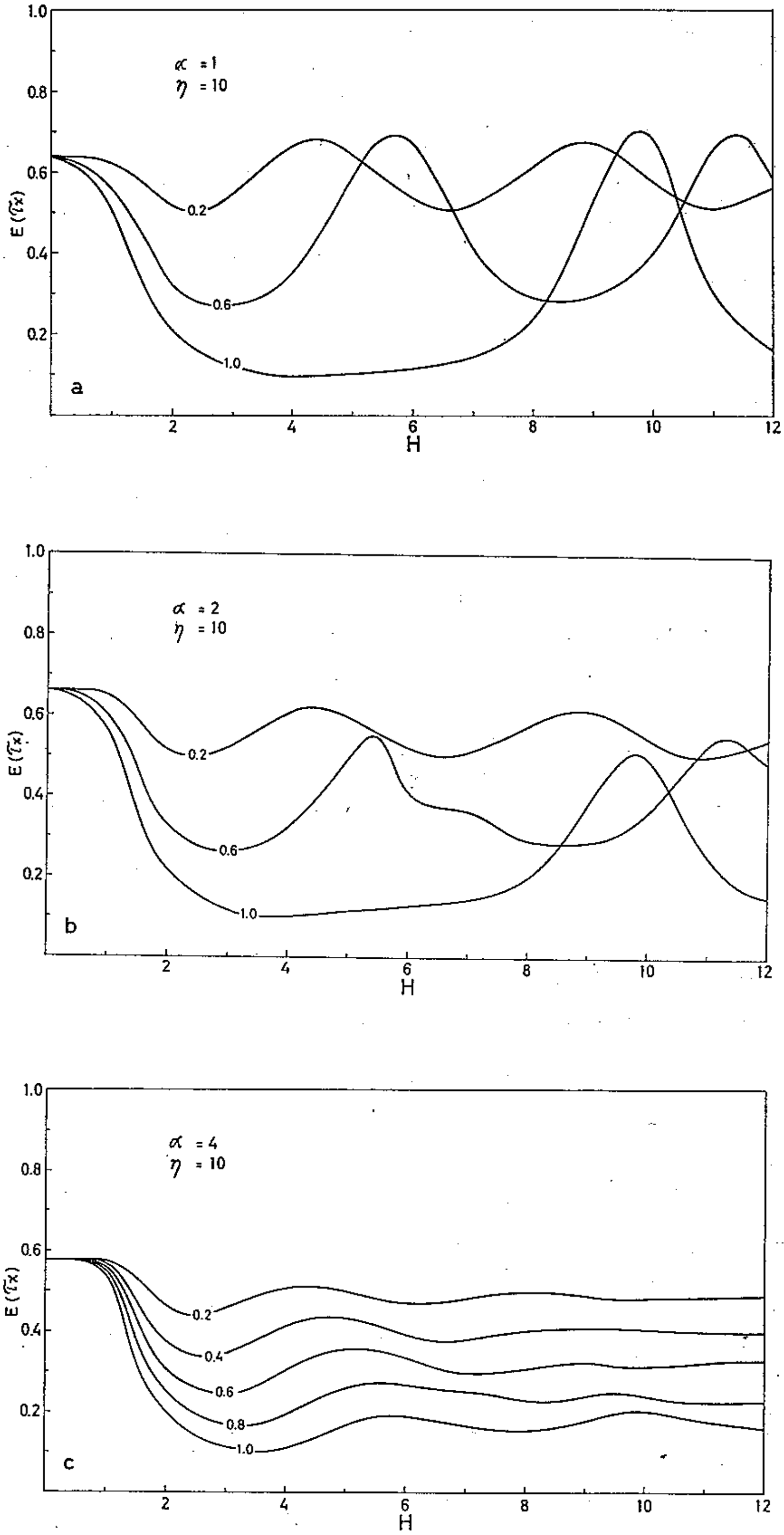

Fig. 5. Same as Fig. 4.

as ε^2 increases (and approaches zero as $l_2 \to \infty$). As a consequence the characteristic tilt of the wave disturbance (e.g. QUENEY, 1947)) becomes less pronounced and therefore less momentum is transported vertically. Some characteristic values of ε^2 are presented in Table 3. The computations have been made assuming a surface temperature of 285 K and mean basic velocities of 20 m sec^{-1} and 30 m sec^{-1} in the lower and upper layers respectively. The curvature of the wind profile was considered negligible and the lapse rates $\gamma^* = \gamma/\gamma_a$ (γ_a is the dry adiabatic lapse rate) were interpreted as mean values.

Table 3. *Characteristic values of* $\varepsilon^2 = l^2{}_2 - l^2{}_1$.

H \ γ^*	0.6	0.7	0.8
8	0.20	0.50	0.88
9	0.22	0.52	0.90
10	0.23	0.54	0.92

The complete expression in (5.3) has been evaluated numerically and the results displayed in Figs. 4a through 5c. (Some intermediate curves have been omitted to enhance the graphical representation.) One of the most striking features is the large amplitude of some of the curves for small values of α and it is possible to have $E(\tau_x) > 1$. This may be explained as a resonance effect which occurs when the vertical wave length of the discrete wave $\xi = 2m\pi/\eta$ is in phase with the interface height H. Mathematically, the resonance occurs when the denominator of the first summation in (5.3) is a minimum, i.e., when

$$\lambda_m H = n\pi \qquad (n = 1, 2, \ldots) \tag{5.4}$$

where $\lambda_m = \sqrt{l_1^2 - (2m\pi/\eta)^2}$ is the vertical wave number of the mth discrete wave. Letting $D_m = 2\pi/\lambda_m$ we obtain

$$\frac{H}{D_m} = \frac{n}{2} \tag{5.5}$$

as the condition for resonance. However we note that when $\eta = 8$ and $\varepsilon^2 = 0.8$, 1.0 ($l_1^2 = 0.6$, 0.5) no resonance peaks appear. For these values of the parameters internal waves only exist in the upper layer and the type of resonance discussed above can not occur, since the upper layer is not bounded from above.

With increasing α the "noise" due to irregularity in the spacing becomes the dominant term and the resonance effect diminishes. When $\alpha = 4$, $E(\tau_x)$ is approximately equal to L/η times the stress due to an isolated mountain; or equivalently, the stress due to an infinite number of mountains spaced a mean distance η apart.

Finally, the "noise" due to irregularities in mountain amplitude is, in general, small compared to the sum of the other terms. An exception occurs in the case when internal waves do not exist in the lower layer ($l_1 < k \leq l_2$); then this "noise" effect is comparable with each of the other contributions when $H > 3$.

6. Expected value of the stress in a three-dimensional atmosphere. CRAPPER (1959) has obtained an approximate solution of (2.8) when u_0 and β^2 are independent of height. The basic current is parallel to the x-axis and flows over the circular mountain

$$h(x,y)=\frac{ar^3}{(x^2+y^2+r^2)^{3/2}}=\frac{ar^2}{2\pi}\int_{-\infty}^{\infty}\int_{-\infty}^{\infty}\exp[-r\sqrt{k^2+l^2}+i(kx+ly)]dldk \tag{6.1}$$

where r is the radius of the mountain at height $a/2^{3/2}$. The character of the solution in planes parallel to the basic current ($y=$ constant) is very similar to the two-dimensional wave solution over a bell-shaped ridge; however since the disturbance has an extra degree of freedom the wave amplitude decays rapidly in the crosswind direction, but the rate of fall-off depends primarily on r.

CRAPPER's model will be used in determining the expected value of the stress[4] for a line of circular mountains oriented (a) parallel to the basic current and (b) crosswind. The wave interactions which occur in (a) are similar to the two dimensional case studied in Section 4. However the introduction of a more realistic mountain profile produces a damping effect on the motion, which reduces the magnitude of the stress below the value in (4.19) as well as insuring that the stress approach zero with u_0. The principal feature which distinguishes case (b) is the effect produced by the infinite spectrum of internal waves which spread out laterally from each mountain. Since there is no physical mechanism for the generation of a critical wave, these waves which differ in phase interfere and account for the rapid fall-off of wave amplitude in the crosswind direction.

6.1 Mountains oriented parallel to the basic current. The center of the first mountain is situated at the origin of the coordinate system ($x=0, y=0$) and its profile is given by (6.1). As in the two-dimensional case the nth mountain downstream is similar in form to (6.1) but is situated at a distance $n\eta+\phi_n$ from the first. The radius r will be the same for each mountain but the amplitude a_n and deviation from the mean spacing ϕ_n are random variables with rectangular probability distributions given by (4.9) through (4.12). The procedure used in Section 4 will now be followed.

The expected value of the drag, in dimensional form, is given by

$$\{\widetilde{D_x}\}_{ave}=2\pi^2\rho_0 u_0^2\int_0^{\beta}\{|\widetilde{F_n(k)}|^2\}_{ave}k^2\sqrt{\beta^2-k^2}\int_{-\infty}^{\infty}\frac{e^{-2r\sqrt{k^2+l^2}}}{\sqrt{k^2+l^2}}dldk \tag{6.2}$$

where $\{|F_n(k)|^2\}_{ave}$ is given by (4.15) with r^2 replacing L. Making the change of variable $l=k\sinh t$ we obtain, with the aid of WATSON (1944, § 6.22, 5),

[4] It can be shown from (2.1), (2.2), (2.3) and (6.1) that the Fourier transform of $v(x,y,z)$ is an odd function of the y-wave number l. Therefore integration over l in the computation of $\tau_y=-\overline{vw}$ yields zero and we need only compute τ_x.

(6.3) $$\{\widetilde{D}_x\}_{ave}=4\pi^2\rho_0 u_0^2 \int_0^{\beta} \{|\widetilde{F_n(k)}|^2\}_{ave} k^2\sqrt{\beta^2-k^2}K_0(2rk)dk$$

where K_0 is the Bessel function of imaginary argument of the second kind.

The "effective area" of the circular mountain will be defined as

(6.4) $$A=r^3\int_{-\infty}^{\infty}\int_{-\infty}^{\infty}\frac{dxdy}{(x^2+y^2+{}^2r)^{3/2}}=2\pi r^2 .$$

Along the perimeter of this circular area, of radius $\sqrt{2}r$, the mountain amplitude is approximately 1/5 its maximum value. When there are $N+1$ mountains the "effective area", displayed in Fig. 6 by the dashed curve, is given by

(6.5) $$A_n=2r(\sqrt{2}N\eta+\pi r)\approx N2\sqrt{2}r\eta .$$

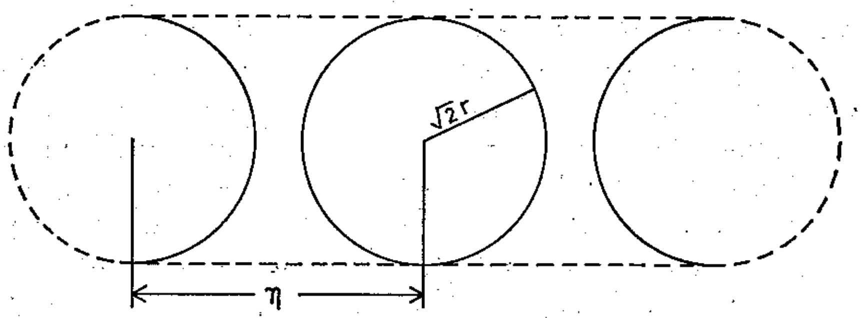

Fig. 6. The dashed line defines the "effective area" of a line of circular mountains spaced a mean distance η apart.

The stress due to an isolated circular mountain ($N=\alpha=a_2-a_1=0$) may be found from (6.3) and (6.4) by letting $k=\beta\cos x$ and using Watson (1944, § 13.72, 4). We obtain

(6.6) $$\tau_x=\rho_0 u_0^2 a^2 r^2 \beta^4 \frac{1}{8}[I_0(\beta r)K_0(\beta r)-I_2(\beta r)K_2(\beta r)]$$

where I_0 is the Bessel function of imaginary argument of the first kind. Recalling that $\beta=v_0/u_0(v_0^2=gd\ln\theta_0/dz)$ we may rewrite (6.6) as

(6.7) $$\tau_x/\rho_0=C_D V_0^2$$

where $C_D=(r^{*2}/8)(I_0(r^*)K_0(r^*)-I_2(r^*)K_2(r^*))$, $r^*=rv_0/u_0$ and the characteristic velocity is $V_0=av_0$. In this form the quantities a and v_0 are held constant in order to display the dependence of τ_x on r and/or u_0. In the following we shall continue to use $\beta=v_0/u_0$ to nondimensionalize (a, r, α, η); however the asterisk designation will be retained as a reminder that *both* u_0 and each of the aforementioned quantities may vary.

The dimensionless quantity C_D is presented as a function of r^* in Fig. 7. The maximum in the curve reflects a "resonance effect" which occurs when the principal

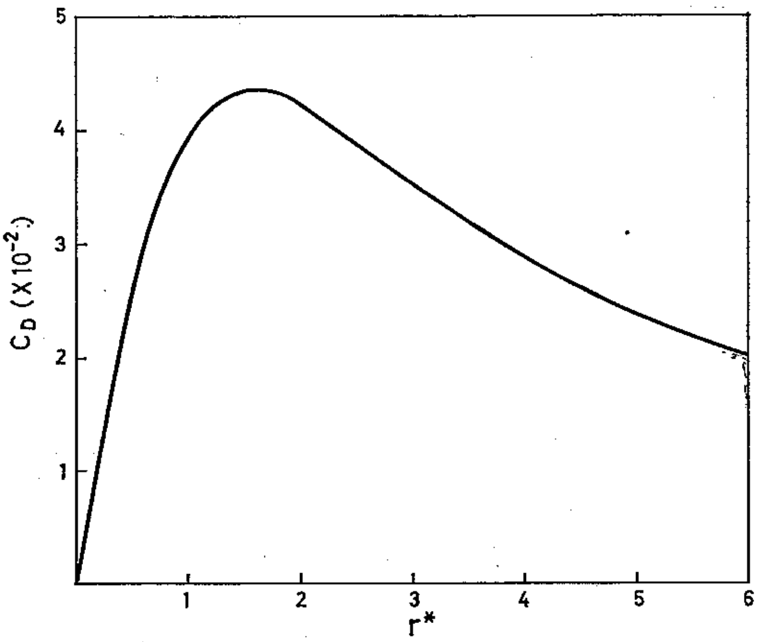

Fig. 7. The nondimensional coefficient C_D as a function of $r^*=rv_0/u_0$ for $v_0=2\times10^{-2}$ sec^{-1}. The maximum occurs at $r^*=1.6$.

Fourier components of the mountain are in phase with those of the solution. CRAPPER (1959) found that the maximum wave amplitude occurs at $r^*=0.6$ in the plane $y=0$; but for increasing values of $|y|$ the maximum amplitude decreases and at the same time occurs at larger values of r^*. This explains why the stress, an integrated quantity, has its maximum at $r^*>0.6$. For $\rho_0=10^{-3}$ gm cm^{-3}, $a=300$ m and $v_0=2\times10^{-2}$ sec^{-1}, the maximum value of τ_x is approximately 16 dynes cm^{-2}. This value, which is considerably below the value in (4.19), reflects the damping effect of a more realistic profile than a point deformation. In addition, values of the stress computed from (6.7) are about the same order of magnitude as estimates of the surface frictional stress over "rugged terrain", which have been compiled by SAWYER (1959).

Using (6.7) as a normalization factor we obtain the expected value of the stress

(6.8) $$E(\tau_x)=\frac{r^{*2}}{C_D}\frac{\sqrt{2}r^*}{\eta^*}\times$$

(i) $$\left\{\frac{2\pi}{\eta^*}\sum_{m=0}^{M}\left(\frac{2m\pi}{\eta^*}\right)^2\sqrt{1-\left(\frac{2m\pi}{n^*}\right)^2}K_0\left(2\frac{2m\pi r^*}{\eta^*}\right)\left(\frac{\sin\frac{2m\pi\alpha^*}{\eta^*}}{\frac{2m\pi\alpha^*}{\eta^*}}\right)^2+\right.$$

(ii) $$\left.\int_0^1\xi^2\sqrt{1-\xi^2}K_0(2r^*\xi)\left[1-\left(\frac{\sin\alpha^*\xi}{\alpha^*\xi}\right)^2\right]d\xi\right\}+$$

(iii) $$\frac{\pi}{2}\frac{\sqrt{2}r^*}{\eta^*}\frac{1}{12}\left(\frac{a_2^*-a_1^*}{\tilde{a}^*}\right)^2.$$

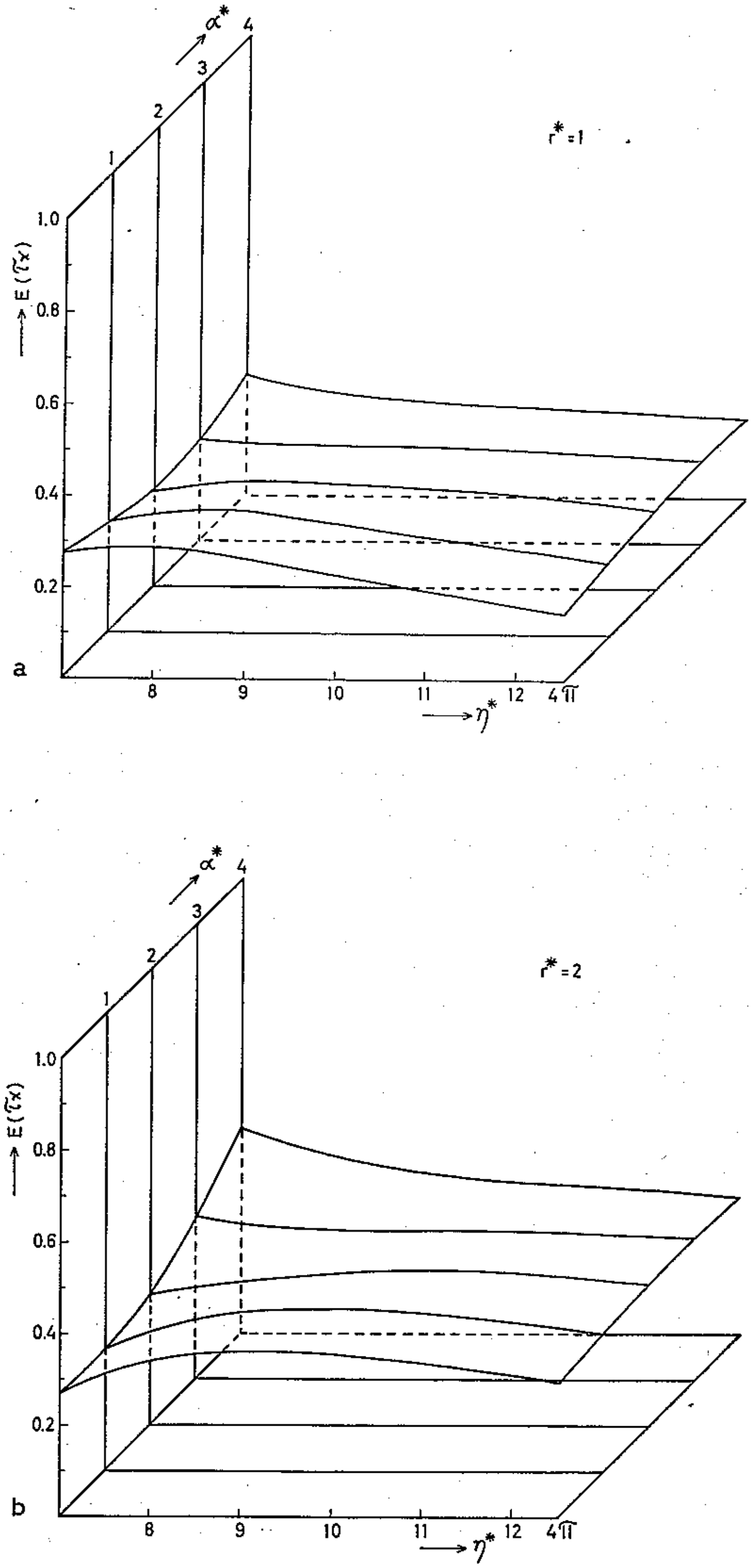

Fig. 8. The expected value of the stress as a function of the mean spacing η^* and deviation α^* for the indicated values of r^*.

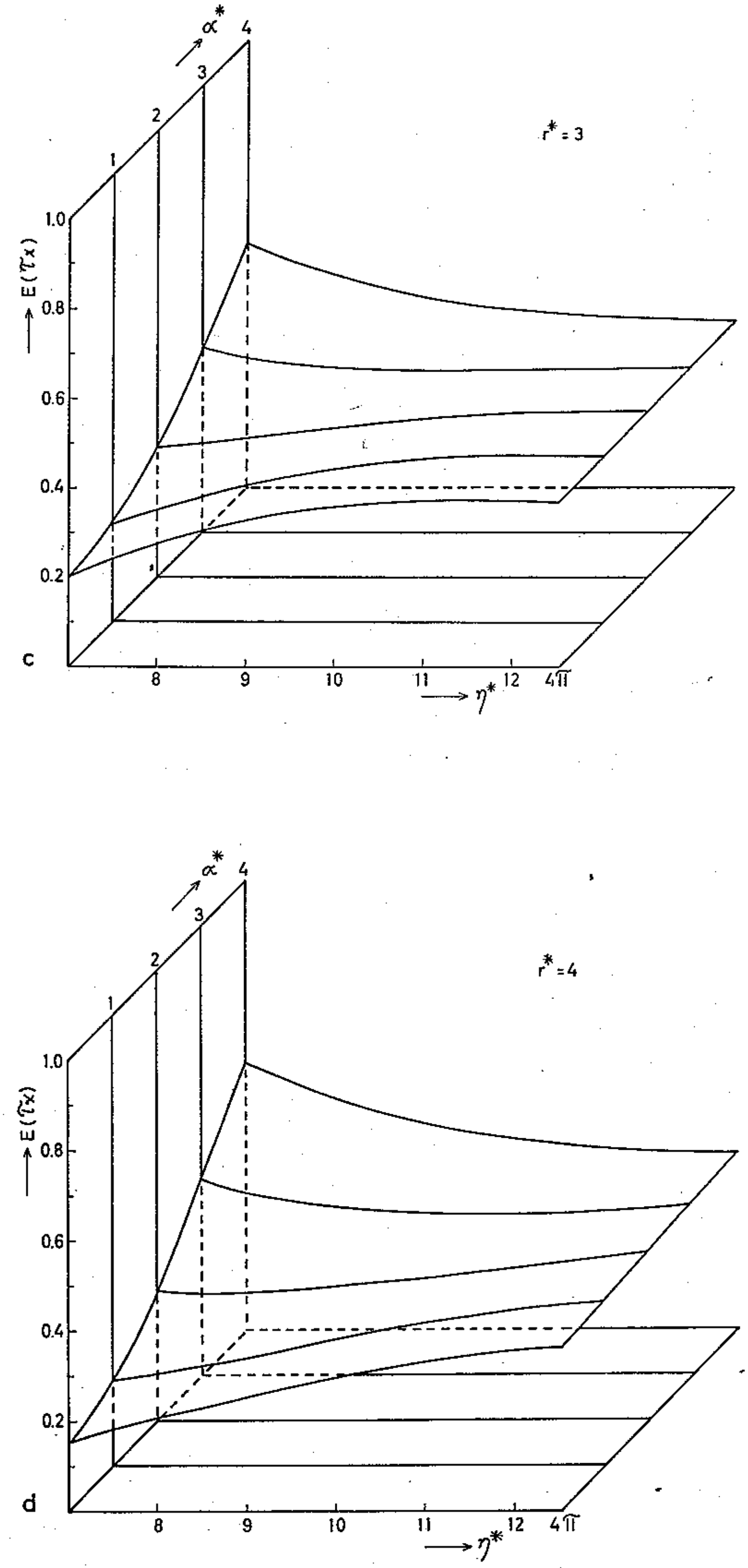
α*
1
2
3
4
r* = 3
1.0
0.8
0.6
0.4
0.2
E(τx)
c
8
9
10
11
12
4π
η*
α*
1
2
3
4
r* = 4
1.0
0.8
0.6
0.4
0.2
E(τx)
d
8
9
10
11
12
4π
η*

Fig. 8.

We note that damping due to the mountain, represented by K_0, is the primary difference between (6.8) and the corresponding terms in (4.23). The results of the numerical computations of $E(\tau_x)$ are displayed in Figs. 8a-d.

The increase of $E(\tau_x)$ for small values of η^* and large values of α^* represents an increase in the "noise" due to variability in the spacing which becomes more pronounced as r^*/η^* increases. When the mountains are widely spaced (r^*/η^* small) this effect is negligible since $E(\tau_x)$ is essentially independent of α^*. The ratio r^*/η^* also affects the discrete contribution (i) and the effect is most noticeable when α^* is small. However when α^* is large and r^* constant, $E(\tau_x)$ decreases approximately like $1/\eta^*$.

6.2 Mountains oriented crosswind. The only difference between this model and that used in (6.1) is the orientation of the $2N+1$ mountains (crosswind). However before letting $N\to\infty$ we must first show that a limit is approached for relatively small values of N. It is sufficient to consider only the contributions from the individual mountains and the interactions between them, since the "noise" terms are essentially independent of N.

An analysis similar to that developed in Section 4 will be followed. The drag due to $2N+1$ circular mountains spaced a mean distance μ apart is represented by

(6.9) $$D_x=2\pi^2\rho_0u_0^2\int_0^\beta k^2\sqrt{\beta^2-k^2}\int_{-\infty}^{\infty}|F_n(l)|^2\frac{e^{-2r\sqrt{k^2+l^2}}}{\sqrt{k^2+l^2}}dl\,dk$$

where

(6.10) $$|F_n(l)|^2=\left(\frac{ar^2}{\pi}\right)^2\left|\sum_{n=-N}^{n=N}e^{-inl\mu}\right|^2=$$
$$(2N+1)+2(2N)\cos l\mu+2(2N-1)\cos 2l\mu+\cdots+2\cos 2Nl\mu\,.$$

The interpretation of (6.9) and (6.10) may be found in the remarks following (4.3). The stress due to $2N+1$ mountains, derived in Appendix C, is given by

(6.11) $$[\tau_x]_n=\frac{\pi}{2}\frac{\sqrt{2}\,r^*}{\mu^*}\left\{1+\frac{2}{2N+1}\frac{1}{C_D^{(0)}}[2NC_D^{(1)}+(2N-1)C_D^{(2)}+\cdots+C_D^{(N)}]\right\}$$

where

(6.12) $$C_D^{(n)}=\frac{r^{*2}}{8}[I_0(\kappa(n))K_0(\kappa(n))-I_2(\kappa(n))K_2(\kappa(n))]$$

and $\kappa(n)=\sqrt{r^{*2}+(n\mu^*/2)^2}$. There is a one-to-one correspondence between the terms in (6.11) and those in (6.10). The results of the numerical computation of (6.11) for $r^*=1$ are presented in Table 4. The limit approached by $[\tau_x]_n$ is given by the column $N=\infty$, computed from (6.13) with $\alpha=a_2-a_1=0$. The last column represents the stress due to the individual mountains. We note that the effect produced by the interactions decreases quite rapidly with increasing μ.

Table 4. *Values of* $[\tau_x]_n$ *for 2N+1 circular mountains,* $N=\infty$ *and when no interactions are present.* $r^*=1$.

N / μ^*	10	15	20	25	∞	$\frac{\pi}{\sqrt{2}}\frac{r^*}{\mu^*}$
π	1.295	1.311	1.317	1.322	1.344	0.706
2π	0.415	0.418	0.418	0.418	0.422	0.353
3π	0.249	0.249	0.249	0.249	0.250	0.235
4π	0.180	0.180	0.180	0.180	0.181	0.178

Since $[\tau_x]_n$ is relatively independent of N we may proceed as before and obtain the expected value of the stress

(6.13)
$$E(\tau_x)=\frac{r^{*2}}{C_D}\frac{\sqrt{2r^*}}{\mu^*}\times$$

(i)
$$\left\{\frac{\pi}{\mu^*}\int_0^1 \xi\sqrt{1-\xi^2}e^{-2r^*\xi}d\xi+\right.$$

$$\frac{2\pi}{\mu^*}\sum_{m=1}^{\infty}\left(\frac{\sin\frac{2m\pi\alpha^*}{\mu^*}}{\frac{2m\pi\alpha^*}{\mu^*}}\right)^2\int_0^1\frac{\xi^2\sqrt{1-\xi^2}}{\sqrt{\xi^2+\left(\frac{2m\pi}{\mu^*}\right)^2}}\exp\left[-2r^*\sqrt{\xi^*+\left(\frac{2m\pi}{\mu^*}\right)^2}\right]d\xi+$$

(ii)
$$\left.\int_0^1\xi^2\sqrt{1-\xi^2}\int_0^\infty\frac{\exp[-2r^*\sqrt{\xi^2+\psi^2}]}{\sqrt{\xi^2+\psi^2}}\left[1-\left(\frac{\sin\alpha^*\psi}{\alpha^*\psi}\right)^2\right]d\psi d\xi\right\}+$$

(iii)
$$\frac{\pi}{2}\frac{\sqrt{2}r^*}{\mu^*}\frac{1}{12}\left(\frac{a_2^*-a_1^*}{\bar{a}^*}\right)^2.$$

There are two contributions to $E(\tau_x)$ in (i): the wave which is independent of $\alpha^*(\psi=0)$ and the infinite discrete spectrum of internal waves which are in phase with the mean mountain spacing μ^*. The contribution from the wave $\psi=0$ is produced by the same Fourier component of each mountain: a ridge extending infinitely far along the y-axis with a bell-shaped variation along the x-axis. This component generates a downstream wave witn no y variation and therefore is unaffected by variations in the mountain spacing[5]. The latter terms in (i) also make a nonzero contribution since the "cut-off" in the internal wave spectrum is absent. In addition the "noise" due to irregularity in the spacing (ii) is a function of the infinite spectrum of internal waves; however

[5] The wave $\xi=\beta^{-1}k=0$ does not contribute to the stress since this Fourier component is independent of x.

the "noise" due to randomness in the amplitude (iii) is independent of the wave number spectrum and does not differ from the corresponding term in (6.8).

When α^* is small the "noise" terms are of order 10^{-1} compared to the contribution from (i). As the irregularity in spacing increases the "noise" due to this effect also increases while the contribution from the discrete spectrum diminishes rapidly. However the contribution from the wave $\psi=0$ remains the dominant term throughout the range of r^* and μ^* used here. Therefore (6.13) has only been evaluated for $\alpha^*=1$. To facilitate the computations $(\sin\alpha^*\psi/\alpha^*\psi)^2$ was expanded as in (4.17), making it possible to perform the integrations explicitly and evaluate (ii) from a finite number of terms of a convergent infinite series. The numerical computations of (6.13) are presented in Table 5, with smallest mean spacing restricted to be the diameter $2\sqrt{2}r^*$ of the "effective area" (6.4).

It is significant that the values of $E(\tau_x)$ in Table 5 are greater than the corresponding values in Figs. 8a-d and become relatively large when the mountains are closely spaced. This result does not seem surprising since the crosswind orientation (particularly the $\psi=0$ component) presents a greater "barrier" to the flow. The role of the interactions between neighboring wave disturbances, for both types of orientation, may be clearly seen by comparing (6.11) with (4.20), for the case $\alpha=0$. $(n\eta)^{-1}(\boldsymbol{H}_0(n\eta)-2(n\eta)^{-1}\boldsymbol{H}_1(n\eta))$ oscillates about zero; hence the interaction terms in (4.20) produce both positive and negative contributions. The interaction terms in (6.11) however always increase the stress.

Table 5. *Expected value of the stress for a line of circular mountains oriented crosswind.* $\alpha^*=1$ and $\mu^*_{\min}=2\sqrt{2}r^*$.

r^* / μ^*	1	2	3	4
π	1.453	—	—	—
2π	0.455	1.488	—	—
3π	0.271	0.611	1.093	—
4π	0.195	0.418	0.698	1.066

7. Concluding remarks. The present calculations may be briefly summarized as follows:

(1) Under the same conditions of wind and stability the stress produced by a ridge or tightly spaced mountains oriented crosswind is greater than the stress produced by a line of mountains oriented parallel to the flow.

(2) In addition the maximum value of the stress occurs when the principal Fourier components of the mountain (or ridge) coincide with the principal components of the wave solution.

(3) If a line of mountains (or ridges) are spaced a mean distance η apart in the down-

stream direction, the effect of the interactions between neighboring wave disturbances depends on the ratio of the mean spacing to the critical wave length L_s. If $\eta/L_s > 1$ there are one or more internal gravity waves which are in phase with the spacing and reinforcement occurs, producing a net stress. However, if $\eta/L_s \leq 1$ all the internal gravity waves are out of phase with the spacing (except the critical wave which does not contribute to the stress) and the net effect of the wave interactions is to cancel the stress due to the individual mountains, producing a zero stress on the atmosphere.

(4) As the mountains become more randomly distributed the critical phase relationships become "blurred" and the stress arises primarily from the individual mountains. This latter result also occurs when the mountains are spaced widely apart.

(5) In general an upper layer, in which $l_2^2 > l_1^2$, (see 5.1), acts to diminish the stress below the value in a reference isothermal atmosphere. However if $\eta/L_s > 1$ there is a resonance effect which occurs when a wave, whose horizontal length is in phase with the mountain spacing, has a vertical wave length which is in phase with the interface (or tropopause) height. Under these conditions the stress may be greater than that produced in the isothermal atmosphere.

If more representative values of the wind and temperature distribution had been incorporated into our models, principal features of the wave solutions would be retained. Therefore it is felt that the results presented above could apply to a wider class of atmospheric conditions than have been treated here. However there are important features of this problem which should be evaluated. In particular, little is known about the effect produced by the flow of air around obstacles; and the flux of momentum during the transient stage of wave development may be of importance, especially in situations where steady-state conditions are never realized. Finally, if the mountains are distributed over an area comparable to the scale of the basic motion the earth's rotation and horizontal variations of the basic current variables should be taken into account.

Acknowledgements. This investigation was initiated at the Massachusetts Institute of Technology under the sponsorship of the National Science Foundation, contract G-18985. It was later carried to completion at the University of Oslo with the generous support of the North Atlantic Treaty Organization Research Grants Programme, contract no. 166. The helpful encouragement offered by N. A. PHILLIPS and A. ELIASSEN throughout this research effort is gratefully appreciated. Thanks are also expressed to S. SPIEGEL for programming some of the numerical computations.

APPENDIX A.

The expected or mean value of $|\sum_{n=0}^{N} a_n e^{-ik(n\eta+\phi_n)}|^2$ is denoted by

$$(A.1)\qquad \left\{|\sum_{n=0}^{N} \widetilde{a_n e^{-ik(n\eta+\phi_n)}}|^2\right\}_{ave} = \left\{\widetilde{\sum_{n=0}^{N} a_n e^{ik(n\eta+\phi_n)} \sum_{m=0}^{M} a_m e^{-ik(m\eta+\phi_m)}}\right\}_{ave} =$$

$$\left\{\sum_{n=0}^{N}\sum_{m=0}^{M} \widetilde{a_n a_m} \cos k(n\eta+\phi_n)\cos k(m\eta+\phi_m)\right\}_{ave} +$$

$$\left\{\sum_{n=0}^{N}\sum_{m=0}^{M} \widetilde{a_n a_m} \sin k(n\eta+\phi_n)\sin k(m\eta+\phi_m)\right\}_{ave}.$$

Using (4.7) and assuming statistical independence between the deviations from the mean, i.e., $\widetilde{(a_n-\tilde{a})(a_m-\tilde{a})}=0$ when $m\neq n$, we obtain

$$(A.2)\qquad \left\{|\sum_{n=0}^{N} \widetilde{a_n} e^{-ik(n\eta+\phi_n)}|^2\right\}_{ave} = \tilde{a}^2\left\{\left[\sum_{n=0}^{N}\cos k(n\eta+\phi_n)\right]^2\right\}_{ave} +$$

$$\tilde{a}^2\left[\left\{\sum_{n=0}^{N}\sin k(n\eta+\phi_n)\right]^2\right\}_{ave} + (N+1)\widetilde{(a_n-\tilde{a})^2}.$$

The following notation will be used:

$$(A.3)\qquad \left\{\sum_{n=0}^{N}[f_n(\phi_n)]^2\right\}_{ave} = \left\{\left[\sum_{n=0}^{N}\cos k(n\eta+\phi_n)\right]^2\right\}_{ave}$$

and

$$\left\{\sum_{n=0}^{N}[g_n(\phi_n)]^2\right\}_{ave} = \left\{\left[\sum_{n=0}^{N}\sin k(n\eta+\phi_n)\right]^2\right\}_{ave}.$$

Then we proceed as above, expanding f_n and g_n into a mean plus a deviation and assuming statistical independence between the deviations. The first term becomes

$$(A.4)\qquad \left\{\sum_{n=0}^{N}[f_n(\phi_n)]^2\right\}_{ave} = \left[\sum_{n=0}^{N}\{f_n(\phi_n)\}_{ave}\right]^2 + \left\{\sum_{n=0}^{N}[f_n(\phi_n)-\{f_n(\phi_n)\}_{ave}]^2\right\}_{ave} =$$

$$\left[\sum_{n=0}^{N}\{f_n(\phi_n)\}_{ave}\right]^2 + \left\{\sum_{n=0}^{N}[f_n(\phi_n)]^2\right\}_{ave} - \sum_{n=0}^{N}[\{f_n(\phi_n)\}_{ave}]^2.$$

It follows that $\left\{\sum_{n=o}^{N}[g_n(\phi_n)]^2\right\}_{ave}$ may be expressed similarly. Returning to the original notation we obtain the result shown in (4.14).

APPENDIX B.

The integral

$$\int_0^1 \xi\sqrt{1-\xi^2}\left(\frac{\sin\alpha\xi}{\alpha\xi}\right)^2 \sum_{m=0}^{\infty} \delta\left(\xi-\frac{2m\pi}{\eta}\right)d\xi \tag{B.1}$$

will be evaluated. First we define a function $g(\xi)$ such that

$$g(\xi)=\begin{cases}\xi\sqrt{1-\xi^2}\left(\dfrac{\sin\alpha\xi}{\alpha\xi}\right)^2 & \text{when } o\leq\xi\leq 1\\ 0 & \text{when } \xi>1\end{cases} \tag{B.2}$$

Then interchanging the order of integration and summation and using (3.6) we obtain

$$\int_0^{\infty} g(\xi)\sum_{m=0}^{\infty}\delta\left(\xi-\frac{2m\pi}{\eta}\right)d\xi=\sum_{m=0}^{\infty} g\left(\frac{2m\pi}{\eta}\right)=\sum_{m=0}^{M}\frac{2m\pi}{\eta}\sqrt{1-\left(\frac{2m\pi}{\eta}\right)^2}\left(\frac{\sin\frac{2m\pi\alpha}{\eta}}{\frac{2m\pi\alpha}{\eta}}\right)^2 \tag{B.3}$$

where M is the largest integer such that $1-(2M\pi/\eta)^2>0$.

APPENDIX C.

Substituting (6.10) into (6.9) and carrying out the integration over $\psi=\beta^{-1}l$, yields

$$D_x=4\pi^2\rho_0u_0^2a^{*2}r^{*4}\int_0^1\xi^2\sqrt{1-\xi^2}\times \tag{C.1}$$

$$\left\{(2N+1)K_0(2r^*\xi)+2(2N)K_0\left(2\sqrt{r^{*2}+\left(\frac{\mu^*}{2}\right)^2}\,\xi\right)+\cdots+2K_0(2\sqrt{r^{*2}+(N\mu^*)^2}\,\xi)\right\}d\xi$$

according to Magnus and Oberhettinger (1949, p. 118). The $2N+1$ integrations in (C. 1) may be performed with the aid of Watson (1944, § 13.72, 4). Then if we define $[\tau_x]_n$ as the normalized value of the stress due to $2N+1$ mountains, we obtain the expression in (6.11).

PRINCIPAL SYMBOLS USED

A	effective area
a	mountain amplitude
a_2-a_1	maximum range of amplitudes
C_D	nondimensional coefficient defined by (6.7)
c_0	adiabatic sound speed
D_x, D_y	x, y components of the drag

$E(\tau_x)$	expected value of the stress
$F(k, l)$	Fourier transform of $h(x, y)$
g	acceleration of gravity
$\boldsymbol{H}_\upsilon$	Struve's function
H	interface height
$h(x, y)$	lower boundary profile
I_υ, K_υ	Bessel functions of imaginary argument
k, l	x, y wave numbers
L	doublet length
L_s	critical wave length $=2\pi/\beta$
l^2	$\beta^2 - u_0^{-1}d^2u_0/dz^2$
$p(\phi)$	probability distribution defined by (4.9) and (4.10)
$q(a)$	probability distribution defined by (4.11) and (4.12)
r	radius of the circular mountain at height $a/2^{3/2}$
u_0	zero-order basic current
u, v, w	$\rho_0^{1/2}(u_1, v_1, w_1)$, (u_1, v_1, w_1) denoting the first-order velocity components
$W(z; k, l)$	Fourier transform of $w(x, y, z)$
x, y, z	rectangular cartesian coordinates
α	maximum deviation from the mean spacing η or μ
Γ	$g/c_0^2 + 1/2d\ln\rho_0/dz$
β	$\upsilon_0/u_0 =$ critical wave number
$\delta(\xi - k)$	Dirac delta function
ε^2	$l_2^2 - l_1^2 =$ difference in l^2 between the upper and lower layers respectively
η, μ	mean spacing between mountains oriented along the x and y axis respectively
υ_0	$(gd\ln\theta_0/dz)^{1/2} =$ Brunt-Väisäla frequency
ξ, ψ	$\beta^{-1}(k, l)$
ρ_0	zero-order density
τ_x, τ_y	x, y components of the stress
ϕ	deviation from the mean mountain spacing η or μ
$\bar{f}$	integration defined by (3.1)
$\{f\}_{ave}$	probability average defined by (4.6)
$\tilde{f}$	probability average defined by (4.8)
g^*	$\beta g =$ nondimensional variable

REFERENCES

CRAPPER, G. D., 1959: A three-dimensional solution for waves in the lee of mountains. *J. Fluid Mech.*, **6**, 51-76.

ELIASSEN, A., and E. PALM, 1961: On the transfer of energy in stationary mountain waves. *Geof. Publ.*, **22**, No. 3, Oslo.

HINES, C. O., 1960: Internal atmospheric gravity waves at ionospheric heights. *Can. J. Phys.*, **38**, 1441-1481.

— 1963: The upper atmosphere in motion. *Quart. J. R. meteor. Soc.*, **89**, 1-42.

LIGHTHILL, M. J., 1959: *Introduction to Fourier analysis and generalized functions.* Cambridge.

MACFARLANE, G. G., 1949: On the energy spectrum of an almost periodic succession of pulses. *Proc. I.R.E.*, **37**, 1139-1143.

MAGNUS, W., and F. OBERHETTINGER, 1949: *Formulas and theorems for the functions of mathematical physics.* (Chelsea Publishing Company, New York).

PALM, E., and A. FOLDVIK, 1960: Contribution to the theory of two-dimensional mountain waves. *Geof. Publ.*, **21**, No. 6, Oslo.

QUENEY, P., 1947: Theory of perturbations in stratified currents with applications to air flow over mountain barriers. *Dept. of Met. of the Univ. of Chicago. Misc. reports* No. 23.

ROBINSON, C., 1948: *A numerical and analytical investigation of Struve's function.* Ph.D. thesis. U. London.

SAWYER, J. S., 1959: The introduction of the effects of topography into methods of numerical forecasting. *Quart. J.R. meteor. Soc.*, **85**, 31-43.

SNEDDON, I. N., 1951: *Fourier transforms.* New York.

WATSON, G. N., 1944: *A treatise on the theory of Bessel functions.* Cambridge.

Avhandlinger som ønskes opptatt i «Geofysiske Publikasjoner», må fremlegges i Videnskaps-Akademiet av et sakkyndig medlem.

Vol. XXI.

No. 1. A. Omholt: Studies on the excitation of aurora borealis II. The forbidden oxygen lines. 1959.
» 2. Tor Hagfors: Investigation of the scattering of radio waves at metric wavelengths in the lower ionosphere. 1959.
» 3. Håkon Mosby: Deep water in the Norwegian Sea. 1959.
» 4. Søren H. H. Larsen: On the scattering of ultraviolet solar radiation in the atmosphere with the ozone absorption considered. 1959.
» 5. Søren H. H. Larsen: Measurements of amospheric ozone at Spitsbergen (78°N) and Tromsø (70°N) during the winter season. 1959.
» 6. Enok Palm and Arne Foldvik: Contribution to the theory of two-dimensional montain waves 1960.
» 7. Kaare Pedersen and Marius Todsen: Some measurements of the micro-structure of fog and stratus-clouds in the Oslo area. 1960.
» 8. Kaare Pedersen: An experiment in numerical prediction of the 500 mb wind field. 1960.
» 9. Eigil Hesstvedt: On the physics of mother of pearl clouds. 1960.

Vol. XXII.

No. 1. L. Harang and K. Malmjord: Drift measurements of the E-layer at Kjeller and Tromsø during the international geophysical year 1957—58. 1960.
» 2. Leiv Harang and Anders Omholt: Luminosity curves of high aurorae. 1960.
» 3. Arnt Eliassen and Enok Palm: On the transfer of energy in stationary mountain waves. 1961.
» 4. Yngvar Gotaas: Mother of pearl clouds over Southern Norway, February 21, 1959. 1961.
» 5. H. Økland: An experiment in numeral integration of the barotropic equation by a quasi-Lagrangian method. 1962.
» 6. L. Vegard: Auroral investigations during the winter seasons 1957/58—1959/60 and their bearing on solar terrestrial relationships. 1961.
» 7. Gunnvald Bøyum: A study of evaporation and heat exchange between the sea surface and the atmosphere. 1962.

Vol. XXIII.

No. 1. Bernt Mæhlum: The sporadic E auroral zone. 1962.
» 2. Bernt Mæhlum: Small scale structure and drift in the sporadic E layer as observed in the auroral zone. 1962.
» 3. L. Harang and K. Malmjord: Determination of drift movements of the ionosphere at high latitudes from radio star scintillations. 1962.
» 4. Eyvind Riis: The stability of Couette-flow in non-stratified and stratified viscous fluids. 1962.
» 5. E. Frogner: Temperature changes on a large scale in the arctic winter stratosphere and their probable effects on the tropospheric circulation. 1962.
» 6. Odd H. Sælen: Studies in the Norwegian Atlantic Current. Part II: Investigations during the years 1954—59 in an area west of Stad. 1963.

Vol. XXIV.

In memory of Vilhelm Bjerknes on the 100th anniversary of his birth. 1962.

Vol. XXV.

No. 1. Kaare Pedersen: On the quantitative precipitation forecasting with a quasi-geostrophic model. 1963.
» 2. Peter Thrane: Perturbations in a baroclinic model atmosphere. 1963.
» 3. Eigil Hesstvedt: On the water vapor content in the high atmosphere. 1964.
» 4. Torbjørn Ellingsen: On periodic motions of an ideal fluid with an elastic boundary. 1964.
» 5. Jonas Ekman Fjeldstad: Internal waves of tidal origin. 1964.
» 6. A. Eftestøl and A. Omholt: Studies on the excitation of N_2 and N_2^+ bands in aurora. 1965.

A.s John Griegs Boktrykkeri